ELSEVIER

Journal of Nuclear Materials 248 (1997) 306–310

journal of nuclear materials

Effects of the solid–solid interface on the thermal behavior of deuterium in zircaloy cladding tubes

I. Takagi *, M. Hashizumi, A. Yamagami, K. Maehara, K. Higashi

Department of Nuclear Engineering, Kyoto University, Yoshida, Sakyo-ku, Kyoto 606, Japan

Abstract

Using nuclear reaction analysis (NRA), experimental studies on diffusion and absorption of hydrogen isotopes in zircaloy were conducted. These thermal behaviors would be influenced by solid–solid interfaces such as zirconium–zircaloy in liner tubes of nuclear fuel elements and impurity–zircaloy on the cladding surfaces. A specimen of Zr-liner Zircaloy-2 cladding was thermally charged with deuterium gas and slowly cooled in the gas. NRA showed that deuterium highly accumulated in the side of zirconium near the interface, and the deuterium concentration in Zircaloy-2 became lower. This indicated that the deuterium redistribution occurred due to the deuterium migration toward the Zr-liner during slow cooling. This redistribution may be explained by a slight difference of temperature dependence of the terminal solubility of deuterium between zirconium and Zircaloy-2. The observed profile of deuterium may suggest the distribution of tritium in stored spent fuel claddings. Another experiment was to observe the deuterium concentration in Zircaloy-4 tubes, of which impurity elements were present on the surface. Before sample specimens were charged with deuterium gas, nickel or iron was deposited in vacuum, mechanically rubbed, or implanted to them. It was found that effects of the impurity–zircaloy interface much depended on the way of impurity charging. © 1997 Elsevier Science B.V.

1. Introduction

Hydriding of zircaloy fuel claddings sometimes causes significant leakage of radioactivity in nuclear power reactors [1]. Solid–solid interfaces of zircaloy and different materials may play an important role of the hydriding. For example, zircaloy claddings with Zr-liner inside have been widely used in water-cooled reactors. If primary hydriding occurs and the gap between UO_2 fuel pellets and the cladding is filled with hydrogen gas [2], zircaloy is indirectly exposed to the gas through the Zr-liner. The zirconium–zircaloy interface would influence the hydrogen distribution in the claddings. In the case of zircaloy claddings without Zr-liner, there may exist some impurities on the surface. The impurity–zircaloy interface would affect the penetration of hydrogen into the claddings. In order to reduce the fuel failures under extended irradiation, it is important to study the effects of these interfaces on the thermal behavior of hydrogen isotopes.

We adopted the nuclear reaction analysis (NRA) technique to obtain the deuterium profiles in metals. In the following section, the radial distribution of deuterium in the Zr-liner claddings which were charged with deuterium in advance will be discussed. In Section 3, experimental results on deuterium profiles in Zircaloy-4 tubes, in which impurities were intentionally introduced on their surfaces, are shown.

2. Deuterium distribution around the zirconium–zircaloy interface

2.1. Zr-liner claddings

Non-irradiated fuel claddings of Zircaloy-2 (Zry-2) with inside liner of zirconium were cut to use as sample specimens. The inner diameter of the original fuel claddings was 10.55 mm, the total wall thickness 0.86 mm, and the

* Corresponding author. Tel.: +81-75 753 5838; fax: +81-75 753 5845; e-mail: takagi@east.nucleng.kyoto-u.ac.jp.

PII S0022-3115(97)00159-1

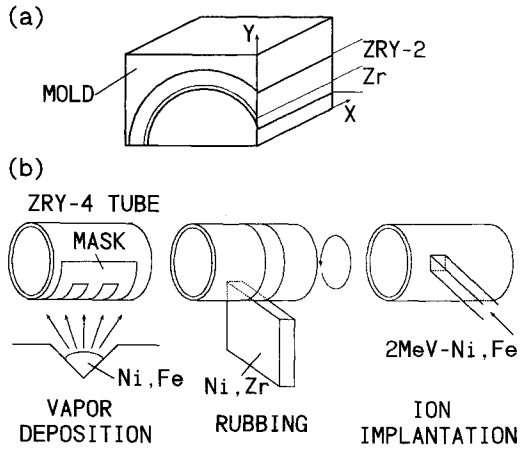

Fig. 1. Sample schematics of (a) Zr-liner cladding and (b) impurity charged Zry-4.

liner thickness about 0.1 mm. Compositions of Zry-2 are Sn (1.28 wt%), Fe (0.16 wt%), Cr (0.11 wt%), Ni (0.06 wt%), O (0.124 wt%) and Zr (balance), and major impurities are C, N, Al and Hf. Zr-liner includes some impurities of Sn (30 wt.ppm), Fe (188 wt.ppm), Cr (23 wt.ppm), Ni (< 50 wt.ppm), and O (400 wt.ppm).

The specimen of 10 mm length was annealed at 853 K for 3 h in a quartz tube under a pressure of $\sim 10^{-4}$ Pa. After the tube was filled with deuterium gas of 0.1 MPa at room temperature, the sample was heated up again and its temperature was kept at 673 K. During this procedure of thermally charging of deuterium, the pressure change in the tube was monitored so as to know the averaged deuterium concentration in the specimen. When the deuterium concentration reached 1 at.%, the charging was stopped. After the charging, one specimen was quenched in water and another was cooled slowly to 433 K at a rate of 60 K/h. As shown in Fig. 1(a), each specimen was buried in a plastic mold and sliced so that a section was parallel to the axis of the tube. The section was mechanically polished with alumina powder.

2.2. Nuclear reaction analysis

In the NRA, a probing beam of 1.3 MeV $^3He^+$ ions from the 4 MeV Van de Graaff accelerator of the Radiation Laboratory, Kyoto University, impinged on the sample at normal to the surface. The beam was cut by two X–Y slits into a rectangular shape with 2 mm width and 50 μm height. The longer side (X-axis) was parallel to the axis of the tube. By moving the sample to the Y-direction, typically with 50 μm steps, the radial distribution of deuterium was observed. As the section plane was apart from the axis of the tube, a 50 μm step corresponded to an about 25 μm step in the radial direction.

The beam current was 1 nA and each measurement required a $^3He^+$ dose of 300 nC. Protons generated from the nuclear reaction $D(^3He, p)^4He$ were detected by a solid-state detector (SSD). The scattering angle was 135° and the solid angle was 14 msr. Aluminum foil of 10 μm thick was placed in front of the SSD to block the penetration of the scattered ^3He particles. The energy spectrum of protons was stored by a multichannel analyzer and converted into the corresponding depth profile of deuterium [3–5]. The maximum probing depth was 1.8 μm.

2.3. Radial distribution of deuterium

Radial distributions of deuterium are shown in Fig. 2. The probed position on the section of the sample was reduced to the radial distance from the inside wall of the cladding tube. In the quenched specimen, the deuterium distribution was uniform from the inside to the outside. The averaged concentration was 1.4 at.%, which agreed with the estimated value from the pressure change. The observed deuterium distribution should be the same as that before quenching since diffusion of deuterium was much restricted after quenching.

In the specimen which was slowly cooled, on the contrary, deuterium accumulated at the side of the Zr-liner near the Zr–zircaloy interface, and the deuterium concentration in the Zry-2 tube became lower (Fig. 2). The peak concentration in Zr-liner was several times as large as that in Zry-2. The decrease of deuterium in Zry-2 was just compensated by the increase in the Zr-liner. This indicated that the deuterium redistribution occurred due to the deuterium migration from Zry-2 tube towards the Zr-liner during slow cooling. It may be suggested that hydrogen

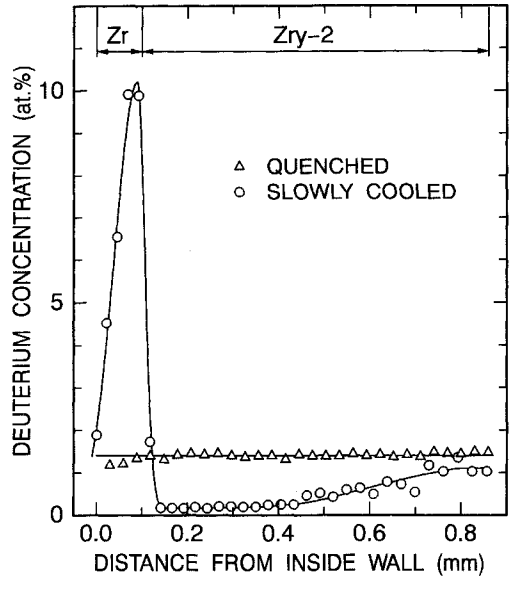

Fig. 2. Radial distributions of deuterium in the Zr-liner zircaloy cladding samples, which were quenched in water and slowly cooled in furnace after deuterium charging.

isotopes in discharged spent fuel will show a characteristic profile near the Zr–zircaloy interface.

The characteristic redistribution can be explained by a small difference of the terminal solid solubility of deuterium between zirconium and Zry-2. During deuterium charging at 673 K, all deuteriums are dissolved in the matrix. Assumed that the terminal solid solubility of deuterium in zirconium is smaller than that in Zry-2 [6], deuteride is formed in zirconium earlier than Zry-2 during slow cooling. Deuteriding would cause a decrease in the dissolved deuterium in Zr-liner and subsequent diffusion of deuterium from Zry-2 to Zr-liner. As the diffusion coefficient is not so large, the deuterium concentration in Zry-2 is lowered only near the interface. Deuterium diffusing into Zr-liner readily forms deuteride and the deuteride concentration near the interface in the Zr-liner increases. When the temperature continues to go down further, deuteride formation begins also in Zry-2. At room temperature, almost all deuteriums exist in the form of immobile deuteride and show the characteristic profile as observed.

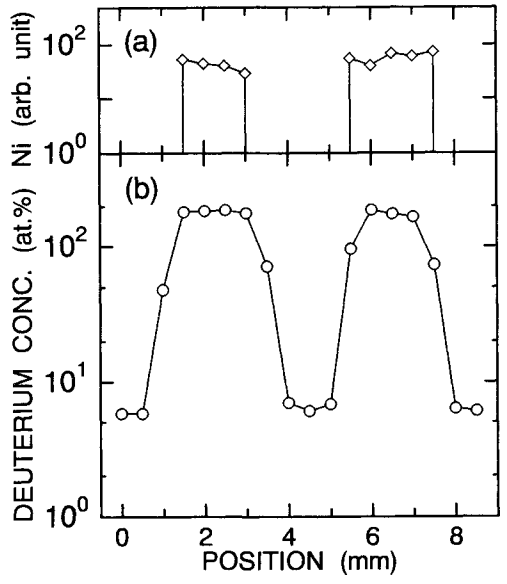

Fig. 3. Concentration profiles of (a) deposited nickel on the surface and (b) absorbed deuterium in the Zircaloy-4 sample.

3. Impurity–zircaloy interface

3.1. Samples and analysis

The outer diameter of the Zircaloy-4 (Zry-4) cladding sample is 9.50 mm and its thickness is 0.63 mm. Its compositions are Sn (1.32 wt%), Fe (0.23 wt%), Cr (0.12 wt%), O (0.13 wt%), C (0.016 wt%) and Zr (balance). The major impurities are N, Al, Si, Ni and Hf.

Some elements were added to the outer surface of the samples as impurities by three ways, that is, vacuum deposition, mechanical rubbing, and ion implantation (Fig. 1(b)). During the deposition, a copper mask with two slits of 2 mm width was put on a sample. The evaporated elements were nickel and iron. The thickness of the deposited layer was around 0.1 μm, estimated from the weight loss of the evaporated material. In the rubbing, a metal plate of 2 mm thick was pressed to a rotating sample for an appropriate time until the color of its surface changed. The plate materials were nickel and zirconium.

In the implantation, nickel and iron ions were accelerated by a Cockcroft–Walton accelerator (the Experimental System for Ion Beam Analysis, Radiation Laboratory, Kyoto University) and perpendicularly impinged on samples. The experimental conditions together with the results estimated by the TRIM code [7] are listed in Table 1. In each case of Ni and Fe, the concentration profile of the implanted ion had a peak at its mean range of 0.9 μm and extended from the surface to its maximum range of 1.6 μm with a FWHM of about 0.6 μm, which was covered by the probing depth of 1.8 μm of the NRA.

Table 1
Conditions and results of the impurity implantation

Ion	Fe^{2+}	Ni^{2+}
Energy	2.0 MeV	
Beam area	3×3 mm^2	
Dose	2.2×10^{20} m^{-2}	1.1×10^{20} m^{-2}
Mean range R_m	0.91 μm	0.86 μm
Maximum range	1.6 μm	1.6 μm
FWHM of profile	0.54 μm	0.57 μm
Concentration at R_m	0.84 at.%	0.42 at.%
Concentration at surface	< 0.01 at.%	< 0.01 at.%

After the impurity addition, each sample was thermally charged with deuterium at 673 K by the same procedure described in Section 2.1. The averaged concentration of absorbed deuterium was a few at.%. The NRA conditions were the same as described in Section 2.2 except for the beam shape of 0.5 mm square. By moving the sample tube along its axis, typically with 0.5 mm steps, the axial distribution of deuterium near the sample surface was observed.

3.2. Effects of impurities

Fig. 3 shows the deuterium distribution in the Ni-deposited sample. The deposited layer has little effect on the NRA measurement, since no changes in the concentration were seen when the layer was removed. The relative concentration of the deposited nickel, measured by PIXE (particle induced X-ray emission), is also shown. The deposited region was almost deuterided while the deuterium concentration in the non-deposited region was lower by two orders magnitude than that in the deposited region. In the case of the Fe-deposited sample, on the other hand,

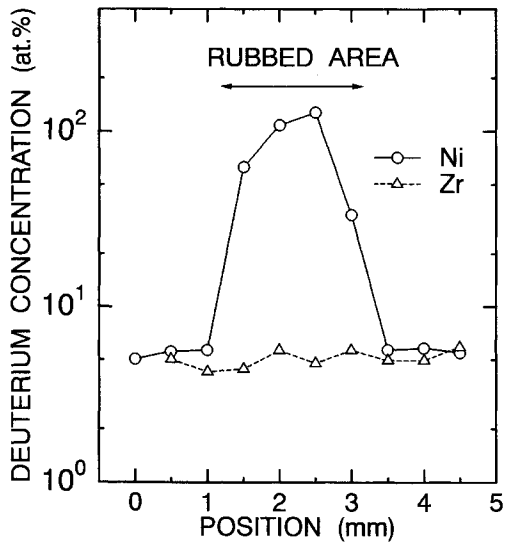

Fig. 4. Deuterium distributions of Ni-rubbed (circles) and Zr-rubbed (triangles) Zircaloy-4 samples.

the deuterium concentration in the deposited region was the same as that in the non-deposited region.

The deuterium distributions in the Ni- and Zr-rubbed samples are shown in Fig. 4. Deuterium highly accumulated in the Ni-rubbed area. The rubbing introduced many scratches on the sample surface. They, however, did not influence on the deuterium concentration since the distribution was almost flat in the Zr-rubbed sample, as shown in Fig. 4.

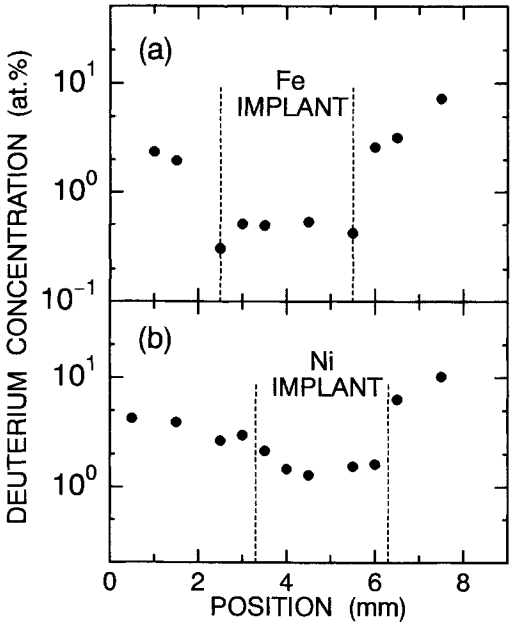

Fig. 5. Deuterium distributions of (a) Fe-implanted and (b) Ni-implanted Zircaloy-4 samples. Conditions of the implantation are listed in Table 1.

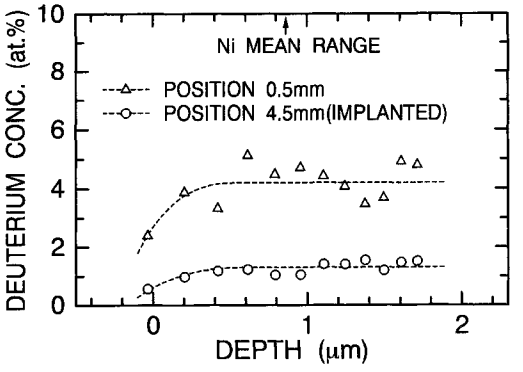

Fig. 6. Depth profiles of deuterium in the Ni-implanted Zircaloy-4 sample. Positions are corresponding to Fig. 5(b).

Another experiment showed that the Zry-4 tube continued to pick up deuterium under our charging condition until it was fully deuterided. So the above results indicated that the rate of deuterium absorption became higher when nickel was present on the sample surface. In other words, surface nickel acted as a window for deuterium uptake.

Fig. 5 shows the deuterium distribution in the (a) Fe- and (b) Ni-implanted samples. The deuterium concentration in the implanted area was lower than that in the non-implanted area. If the implanted elements of Ni and Fe changed some bulk properties concerned with hydrogen, the deuterium concentration should become lower near the mean range of 0.9 μm. The depth profiles of deuterium in the implanted area was, however, almost flat from the surface to the probing depth of 1.8 μm as shown in Fig. 6. So the decrease in the deuterium concentration would be caused by a decrease in the deuterium absorption rate and be attributed to some changes in the sample surface.

The ion implantation would change the surface in various ways. The addition of surface impurities as observed in the Ni-deposited and the Ni-rubbed samples, however, was not effective because the TRIM calculation shows that few ions were present near the sample surface (< 0.01 at.%, see Table 1). About ten atomic layers would be sputtered assuming a typical sputtering yield of 1 [8]. The sputter cleaning generally removes surface oxide layers and tends to enhance the deuterium absorption, which contradicts the experimental results. So sputtering effects would not be responsible. Irradiation effects such as radiation defects and ion mixing might alter surface properties concerned with hydrogen but there is little information about them and further researches are needed.

In this experiment of the zircaloy–impurity interface, it was revealed that the way of impurity charging strongly

affected the absorption rate of hydrogen isotopes, that is, the hydrogen concentration in the zircaloy claddings.

4. Summary

Using the nuclear reaction analysis (NRA), deuterium concentrations were observed in zircaloy claddings, in which deuterium was thermally charged in advance. In the Zr-liner Zircaloy-2 claddings, which were cooled slowly after deuterium charging, deuterium migrated from Zircaloy-2 claddings to Zr-liner, and deuterium redistribution occurred near the Zr–zircaloy interface. This may be explained by a small difference of the terminal solid solubility in zirconium and Zircaloy-2.

In the Zircaloy-4 claddings with some impurities on their surfaces, the deuterium absorption rate depended on the way of impurity charging. For example, the deposition and the rubbing of nickel enhanced the deuterium absorption markedly, while the implantation of nickel did not. The deposition of iron had no effects but the iron implantation suppressed the deuterium absorption.

The above results suggest that the solid–solid interfaces and the existence of impurities on surface would play important roles for the thermal behaviors of hydrogen isotopes in nuclear fuel claddings and possibly for their secondary hydriding.

Acknowledgements

This work was supported in part by a grant-in-aid for scientific research from the Ministry of Education, Science and Culture, Japan. We are grateful to H. Fujita, K. Yoshida, K. Norizawa and M. Naitoh for their support in the ion beam analysis.

References

[1] F. Garzarolli, R. Jan, H. Stehle, Atom. Ener. Rev. 17 (1979) 13.
[2] D.H. Locke, IAEA Specialists' Meeting on Behavior of Defected Zirconium Alloy Fuel in Water Reactors, Chalk River, Canada, Sept. 1979, IAEA Document No. IWGFPT/6 (1980) 101.
[3] D. Dieumegard, D. Dubreuil, G. Amsel, Nucl. Instrum. Meth. 166 (1979) 431.
[4] C.J. Altstetter, R. Behrisch, J. Bøttiger, F. Pohl, B.M.U. Scherzer, Nucl. Instrum. Meth. 149 (1978) 59.
[5] J.L. Yarnell, R.H. Lovberg, W.R. Stratton, Phys. Rev. 90 (1953) 292.
[6] J.J. Kearns, J. Nucl. Mater. 22 (1967) 292.
[7] J.F. Ziegler, J.P. Biersack and U. Littmark, The Stopping and Range of Ions in Solids (Pergamon, New York, 1985).
[8] N. Matsunami et al., Energy dependence of the yields of ion-induced sputtering of monoatomic solids, Institute of Plasma Physics, Nagoya University, IPPJ AM-32, 1983.